

The diurnal cycle of shallow Cumulus clouds over land: A single column model intercomparison study

By Geert Lenderink^{1*}, A. Pier Siebesma¹, Sylvain Cheinet², Sarah Irons³, Colin G. Jones⁴, Pascal Marquet⁵, Frank Müller⁶, Dolores Olmeda⁷, Javier Calvo⁷, Enrique Sanchez⁷, and Pedro M. M. Soares^{8,9}

¹*Royal Netherlands Meteorological Institute, The Netherlands*

²*Laboratoire de Meteorologie Dynamique, Paris, France*

³*Met Office, Bracknell, Berkshire, United Kingdom*

⁴*Rosby Center, SMHI, Norrköping, Sweden*

⁵*Météo France (CNRM/GMGEC), Toulouse, France*

⁶*Max-Planck Institut für Meteorologie, Hamburg, Germany*

⁷*Instituto Nacional de Meteorologia, Madrid, Spain*

⁸*DECivil, Instituto Superior de Engenharia de Lisboa, Portugal*

⁹*Centro de Geofísica da Universidade de Lisboa, Portugal*

(Received 1 July 2003; revised 31 January 2004)

SUMMARY

An intercomparison study for single column models (SCMs) of the diurnal cycle of shallow cumulus convection is reported. The case, based on measurements at the ARM Southern Great Plain site on 21st June 1997, has been used in an LES intercomparison study before. Results of the SCMs reveal the following general deficiencies: too large values of cloud cover and cloud liquid water, unrealistic thermodynamic profiles, and high amounts of numerical noise. Results are also strongly dependent on vertical resolution

These results are analyzed in terms of the behavior of the different parameterization schemes involved: the convection scheme, the turbulence scheme, and the cloud scheme. In general the behavior of the SCMs can be grouped in two different classes: one class with too strong mixing by the turbulence scheme, the other class with too strong activity by the convection scheme. The coupling between (subcloud) turbulence and the convection scheme plays a crucial role. Finally, (in part) motivated by these results several models have been successfully updated with new parameterization schemes and/or their present schemes have been successfully modified.

KEYWORDS: boundary-layer clouds EUROCS

1. INTRODUCTION

The representation of clouds in present Atmospheric General Circulation Models (AGCMs) used in climate research and in numerical weather prediction (NWP) is relatively poor, thereby limiting the predictability of cloud feedbacks in a changing climate. In particular, the representation of shallow cumulus (Cu) convection is an important issue. Shallow cumulus clouds are an integral part of the Hadley circulation, increasing the near surface transport of moisture to the ITCZ, thereby intensifying deep convection (Tiedtke 1989). Over land, shallow cumulus convection also plays an important role in the preconditioning for deep convection.

For these reasons shallow cumulus convection has been the subject of many studies, in particular in Working Group 1 (WG-1) of GCSS [GEWEX (Global Energy Water cycle EXperiment) Clouds System Study (Browning 1993)]. In the 4th GCSS WG-1 intercomparison case (“BOMEX”) a typical tradewind shallow Cumulus cloud with low cloud fraction was studied (Siebesma *et al.* 2003). The next case (“ATEX”) concentrated on cumulus clouds rising into stratocumulus (Stevens *et al.* 2001), which is a common cloud regime in the tradewind area near the transition from stratocumulus clouds to cumulus clouds (de Roode and

* Corresponding author: Royal Netherlands Meteorological Institute, De Bilt, 3730 AE, The Netherlands
© Royal Meteorological Society, 2002.

Duynkerke 1997). Finally, the 6th GCSS WG-1 case (“ARM”) focused on the diurnal cycle of cumulus clouds over land (Brown *et al.* 2002).

In all these intercomparisons, the main emphasis was on the comparison of LES results with observations, and the intercomparison of the different LES results. This has been extremely helpful in evaluating the different LES models, giving confidence that LES can be used for these cases as a “substitute” (but no replacement) of reality providing us with a full 3D picture of the turbulent motions where measurements are sparse. This also opens a way to critically evaluate the different parameterizations involved with the representation of convective clouds, like e.g. mass flux schemes and cloud schemes. In particular, the BOMEX case has been very popular in this respect (e.g., Siebesma and Cuijpers 1995; Siebesma and Holtslag 1996; Grant and Brown 1999; Bechtold *et al.* 2001; van Salzen and McFarlane 2002; Neggers *et al.* 2002).

Despite this, relatively little attention has been paid to the critical evaluation and documentation of results from single column models (SCMs) derived from (semi-) operational NWP or climate models. In the last few years, however, it has become clear that this step is essential, and that the whole cycle of intercomparing observations, LES and SCMs (and full 3D AGCM simulations) is critical to actually improve parameterizations in operational models.

This paper studies the representation of the diurnal cycle of cumulus convection in several SCM versions of (semi-)operational models. We use the GCSS WG-1 6th case studying the diurnal cycle of Cumulus clouds (Brown *et al.* 2002) for the following reason. This case is rather demanding because all the parameterizations in the SCM have to work together in the different regimes capturing the diurnal cycle. What might work well in the mature stage of Cu clouds might not work properly in other stages of the diurnal cycle. Further, many of the parameterizations recently developed have been tuned to the stationary marine BOMEX case, and it is not clear how well they work for this nonstationary continental case.

The first objective of the paper is to show how realistic cumulus clouds are represented by state-of-the-art, operational climate/NWP models. The models considered are: ARPEGE (CLIMAT), ECHAM4, the ECMWF model (hereafter shortly denoted ECMWF), HIRLAM, MESO-NH, RACMO and the UK Met Office model (hereafter METO). These models are described in the Appendix (see also table 1). The second objective is to analyze the behavior of the different parameterization schemes involved. These are the turbulence scheme, the convection scheme and the cloud/condensation scheme. We will keep this analysis as general as possible, not focusing too much into the behavior of one particular model, but attempting to identify typical behavior in classes of models/or parameterizations. In this respect, it is explicitly mentioned that it is not our purpose to distinguish between good and bad *models*. One bad assumption or bad scheme might jeopardize the solution of an otherwise good model, and relatively good results might be obtained through canceling errors. As part of the analysis we will also show some results of research models, that are not (yet) in operational use, in order to illuminate our findings further. Finally, (in part) motivated by these results several models have been successfully updated with new parameterization schemes and/or their present schemes have been successfully modified. The outcome of these improvements is also documented here. This comparison is part of the EU-funded EUROCS (European Cloud Systems) project, which aims at improving the representation of clouds in climate models.

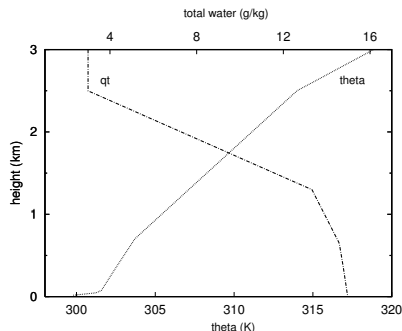


Figure 1. Initial profiles of potential temperature θ (K) and total water q_t (g kg^{-1}).

2. CASE

(a) Case Description

The case is based on an idealization of observations made at the ARM Southern Great Plains (SGP) site on 21st June 1997. During that day cumulus clouds developed on top of a clear convective boundary layer. The case was compiled by Andy Brown of the UK Met Office and is described in detail in Brown *et al.* (2002).

The initial profiles are shown in Fig. 1. The surface latent and sensible heat fluxes are prescribed, with values close to zero in early morning and the evening, and a maximum at midday of 500 W m^{-2} and 140 W m^{-2} , respectively. This implies a Bowen ratio of approximately 0.3, whereas typical values in marine Cu are much lower (e.g., 0.06 in BOMEX). Small tendencies representing the effect of large-scale advection and shortwave radiation are prescribed [for details see Brown *et al.* (2002)].

(b) Summary of LES results

In Brown *et al.* (2002) the results of 8 LES models are discussed. The spread between these different LES results was relatively small, in particular in comparison with the spread in the SCM results presented here. For convenience, we will therefore only present LES results of the KNMI LES model (Cuijpers and Duynkerke 1993).

In Fig. 2 the evolution of the potential temperature and the cloud liquid water in the LES is shown. The evolution of the potential temperature reveals the growth of the inversion from near the surface to 800 m at 15 UTC (9 LT) when clouds appear. At that time clouds are shallow with the highest cloud tops at 1000-1500 m, but gradually the cloud layer deepens with the highest cloud tops at 2500-2800 m after 19 UTC (13 LT). At the same time cloud base rises from 800 m to 1300 m. Values of cloud liquid water (domain averaged) are relatively low with values of $0.01\text{-}0.04 \text{ g kg}^{-1}$.

Other LES results are shown in concert with the SCM results. We will focus mainly on time series of Liquid Water Path (LWP) and cloud fraction, and on the vertical profiles at two different stages: at 17.30 UTC with a shallow cloud layer forced from the subcloud and at 21.30 UTC with well developed, active clouds.

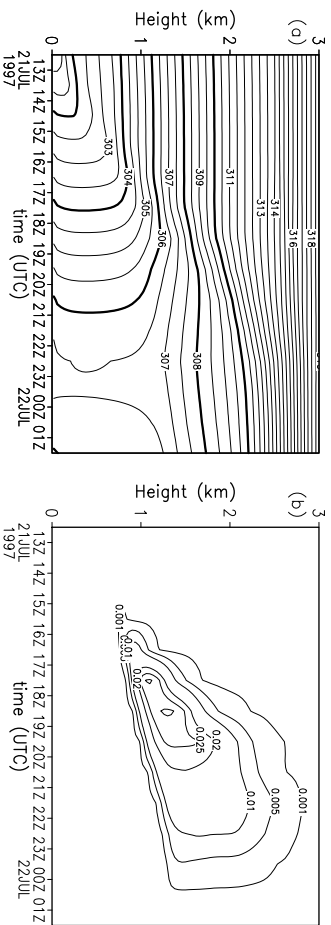


Figure 2. Time evolution of the potential temperature and cloud liquid water in the KNMI LES model. Contour interval 1 K and 0.005 g kg^{-1} , with an additional contour at 0.001 g kg^{-1} .

3. RESULTS OF THE (SEMI-) OPERATIONAL VERSIONS

We intercompare results of 7 different models: ARPEGE (CLIMAT), ECHAM4, ECMWF, HIRLAM, METO, Meso-NH and RACMO. For METO only the mean profiles and the timeseries were available. These models and their physics packages are shortly described in the appendix. Some relevant model aspects are also described in concert with the analysis of the results.

Most participants have run their model on two different vertical resolutions, R_{19} and R_{40} with respectively 19 and 40 levels in the lowest 4 km of the atmosphere. Resolution R_{19} equals (in the lowest 4 km) the L60 resolution presently operational in ECMWF (Teixeira 1999). R_{19} has a vertical grid spacing of 200-400 m in the cloud layer (and higher near the surface). Even though R_{19} is at present a high operational resolution, the cloud layer is only resolved by 3 or 4 points, and numerical errors are relative large. Therefore, we also requested R_{40} with a grid spacing of 150-200 m in the cloud layer. If available, we therefore show results on R_{40} . For ECMWF and HIRLAM we show results on R_{19} since results on R_{40} were not available. It is noted here that in ECHAM4 and METO results on R_{40} are rather different from results on the lower vertical resolution at which the model is run operationally. Sensitivity to vertical resolution will be shown in section 5(c).

(a) Timeseries

In Fig. 3 the time evolution of the total (projected) cloud cover is shown. Most models have too high cloud cover in the mid-afternoon, over 50 % in ECMWF, ECHAM4, ARPEGE and HIRLAM. In addition, in most models clouds do not dissolve at the end of the day (HIRLAM, RACMO, ECMWF, ECHAM4), or even peak in cloud fraction after sunset (RACMO and HIRLAM). ECHAM4 already has a rather high cloud cover in the early hours of the simulation.

It is not entirely trivial to compare total projected cloud cover in the SCMs and in the LES. Both LES and SCM predict a cloud fraction at each model height (see e.g. Fig. 5). The total cloud cover is defined as the vertical projection of the 3D cloud field onto the surface. Because in the LES the full 3D cloud field is available, the projected cloud cover can be computed; in the LES the projected cloud cover is a factor 2 larger than the maximum of the cloud fraction profile. However, in the SCMs a full 3D cloud field is not available and a cloud

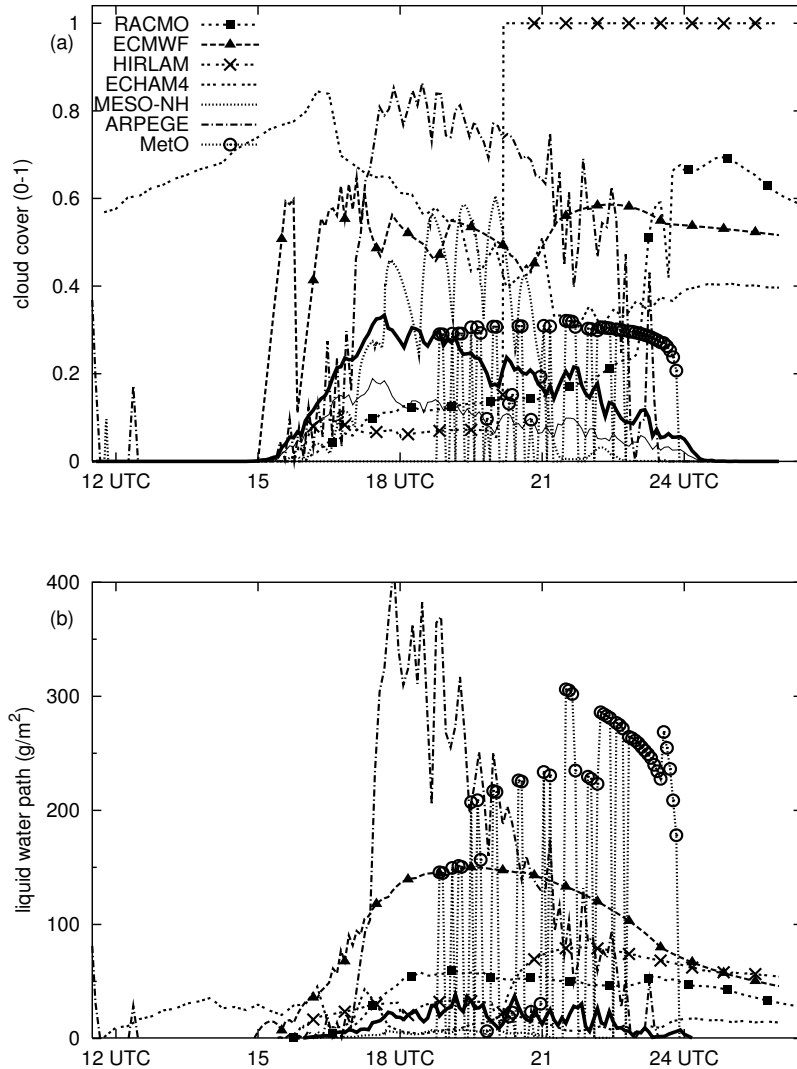


Figure 3. Time series of cloud cover (0-1) and cloud liquid water path (g m^{-2}). The LES results for total cloud cover (thick solid line) and maximum cloud fraction (thin line).

overlap assumption has to be made. With the common assumption of maximum random overlap and the LES profile in Fig. 5 the projected cloud cover would equal the maximum of cloud fraction profile, and the cloud cover would therefore be underestimated. On the other hand, ARPEGE produces a cloud cover far exceeding the maximum of the cloud fraction profile (in Fig. 5) since the cloud overlap assumption effectively treats the different maxima in the cloud fraction profile as separate (independent) cloud layers.

The cloud liquid water path (vertical integral of the mean liquid water content) shows similar behavior. Most SCMs have LWPs that are a factor 2-5

times higher than in the LES model, most outspoken in ARPEGE and METO with values over 300 g m^{-2} , and in ECMWF reaching 150 g m^{-2} . In both LWP as in cloud cover most SCMs show a high level of intermittency. Note that the intermittency in the LES results is caused by sampling of a relatively small amount of clouds in the LES domain of $6.4 \times 6.4 \text{ km}$. Most SCMs, however, are representative for (much) larger domain sizes, and the parameterizations do not explicitly represent the lifecycle of a single cloud and therefore should not contain this type of intermittency.

(b) *Profiles*

Profiles at 17.30 UTC just after the onset of clouds are shown in Fig. 4. In the LES model there is a shallow cloud layer with cloud base at 800 m and highest cloud tops at 1500 m. There is no well developed conditionally unstable profile yet as can be seen in (mean) profiles of total water q_t and the potential temperature θ (which in this case is close to the liquid water potential temperature θ_l since the cloud liquid water content is small). In this phase, the clouds are mainly forced from the subcloud layer. The profiles of θ and q_t in the SCMs are reasonably close to the LES results. Some SCMs, however, already developed a considerable amount of grid point noise, in particular in ECHAM4 (see e.g. results for q_t , relative humidity and u). At this early stage of cloud formation, the cloud fraction and cloud liquid water already show rather high values in most SCMs (except in HIRLAM and METO which have no clouds at this time). In the LES model the shape of profiles of liquid water and cloud fraction is similar, but in the SCMs they are often rather dissimilar. For example, ECHAM4 has clouds reaching the surface, but no correspond liquid water, and in ECMWF liquid water strongly peaks at one layer in the inversion, but the cloud layer extends over more layers. MESO-NH has a rather high cloud fraction (45 %) but almost no corresponding liquid water. RACMO shows the opposite behavior, with somewhat low cloud fractions, but too much cloud liquid water. ECHAM4 and RACMO have unrealistic wind profiles with a strong minimum in u in the cloud layer. ECMWF has too strong winds in the sub-cloud layer.

The profiles at 21.30 UTC (15.30 local time) are shown in Fig. 5. The differences between the LES model and the SCMs, and among the different SCMs have increased significantly. Four models (ECMWF, ARPEGE, ECHAM4, and METO) have high moisture contents near the inversion above 2000 m, whereas the lower part of the cloud layer, in particular near cloud base, is too dry. ECMWF and ECHAM4 are too warm in the lower part of the cloud layer, with a (strong) inversion at cloud base. On the other hand, the profiles of potential temperature in ARPEGE and METO are too well mixed in the cloud layer. HIRLAM is characterized by a very shallow boundary layer, which is too moist and covered with thick stratiform clouds. The temperature and moisture profiles in RACMO and MESO-NH are reasonably close to the LES results (see e.g. the profile of relative humidity), but the cloud fraction in MESO-NH is too small and the cloud liquid water in RACMO too large. ECMWF has a remarkable peak in cloud fraction in the inversion, despite that the relative humidity at that height is below 80 %. A peak in cloud fraction in ARPEGE at 2500 m corresponds to a maximum in relative humidity (90 %) at that height. Noise is apparent in the profiles of ECHAM4 and to a lesser extent in ARPEGE. [Note that e.g. ECHAM4 seems to have problems with conserving heat or did not apply the correct forcing since they are too warm (compared to LES) everywhere.]

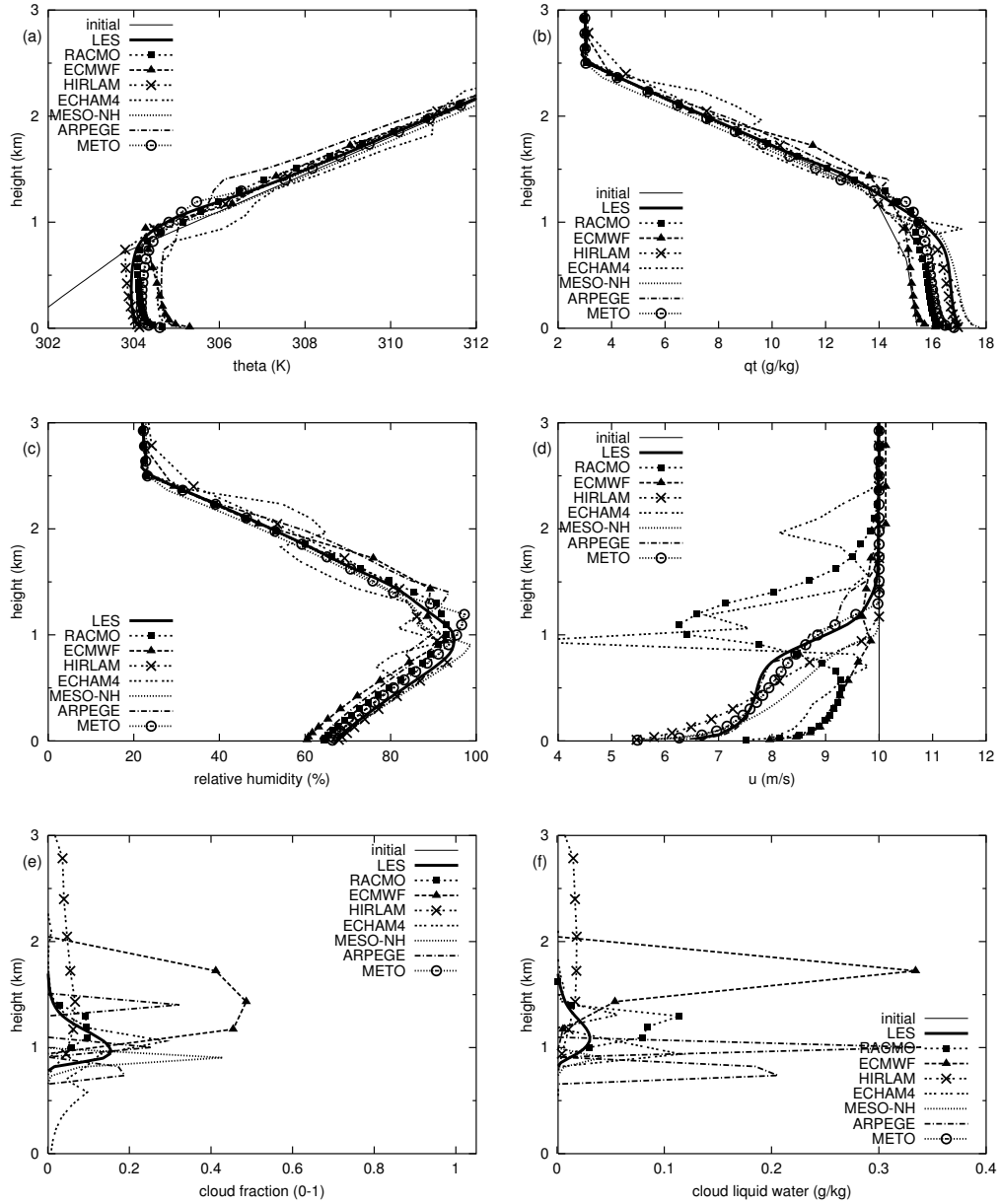


Figure 4. Profiles of potential temperature θ (K), total water q_t (g kg^{-1}), relative humidity (%), horizontal velocity u (ms^{-1}), cloud fraction and cloud liquid water q_l (g kg^{-1}) at 17.30 UTC (11.30 LT). LES results are hourly averages; SCM results are instantaneous values. The thin solid lines denote the initial profiles.

In four models the clouds did not dissolve at the end of the day. Fig. 6 shows the relative humidity and cloud fraction in the evening 19.30 local time at a time when the cloud should have disappeared. RACMO and HIRLAM are close to saturation just below the inversion, and accordingly predict high cloud fractions. In ECMWF the cloud fraction peaks close to the inversion at a higher

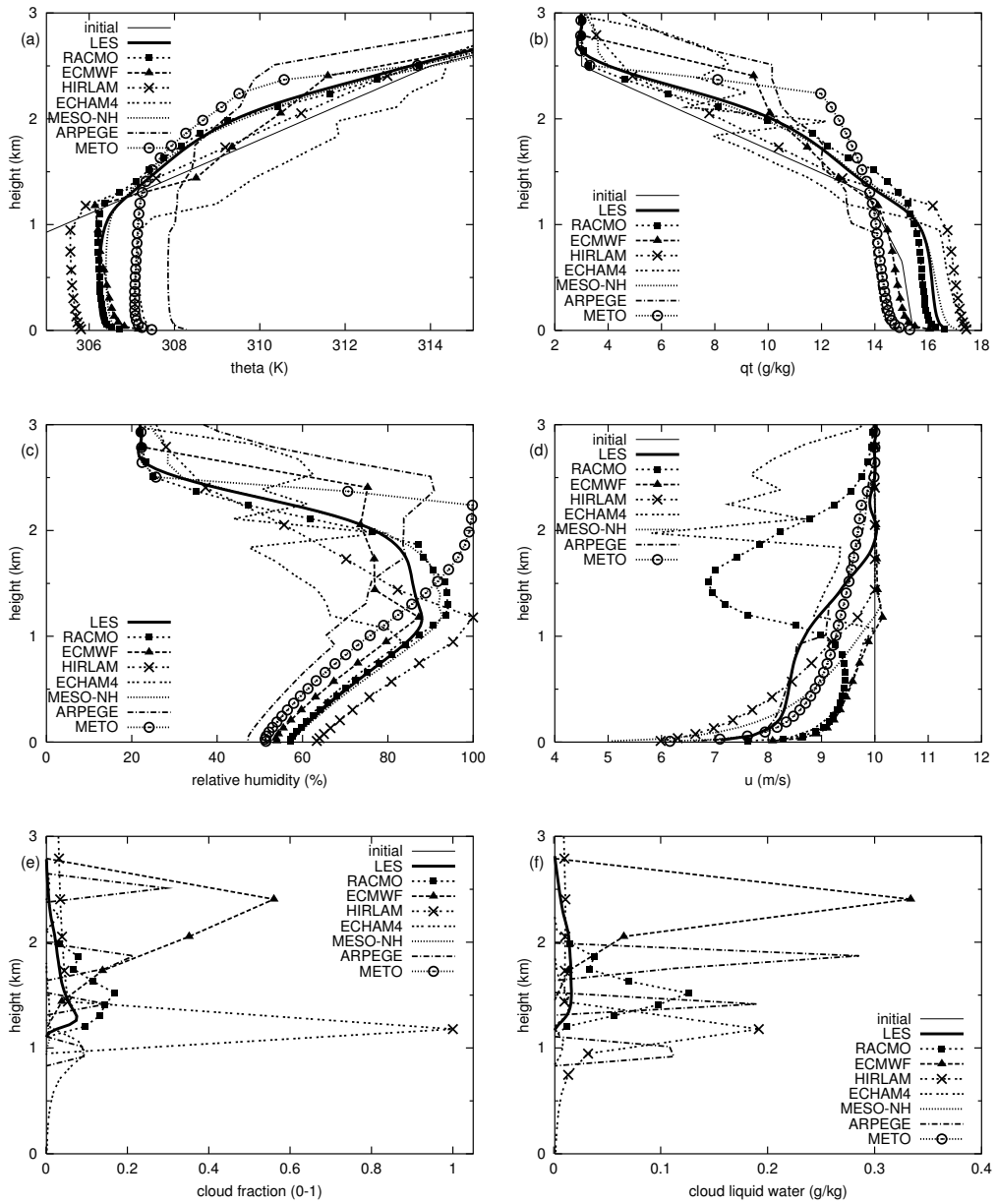


Figure 5. As Fig. 4 but now at 21.30 UTC (15.30 LT). Note that these are instantaneous values. In models with intermittent behavior this may be rather different from the time averaged results. For example, METO has no cloud at this time, whereas from the time series it is clear that there are clouds in the time mean values.

level. In ECHAM4 some thin clouds remain, despite the comparatively low relative humidity.

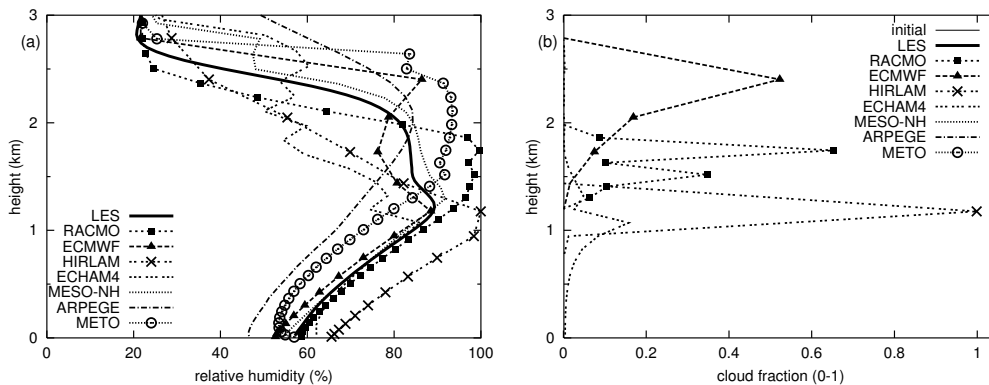


Figure 6. Profiles of relative humidity and cloud fraction at 1.30 UTC (19.30 LT)

4. ANALYSIS OF THE RESULTS

The results are analyzed in terms of the individual behavior of the different parameterization schemes and their mutual interaction. As discussed in the introduction, three parameterizations play a major role: *i*) the turbulence scheme, *ii*) the convection scheme, and *iii*) the cloud/condensation scheme.

(a) Turbulence

All models use diffusion to represent subcloud turbulent mixing; that is, the turbulence scheme computes fluxes from

$$\overline{w'\phi'}_{turb} = -K\phi \frac{\partial\phi}{\partial z}, \quad (1)$$

where $\phi = \{u, v, \theta, q, \text{etc}\}$. Here, and in the following, ϕ denotes the grid box mean value. Commonly used closures to compute the eddy diffusivity K are the TKE- l closure, the Louis (1979) closure, or the K -profile method (Troen and Mahrt 1986). Except METO none of the models use a nonlocal transport term (such as e.g. proposed by Holtslag and Boville 1993).

The TKE- l scheme employs a prognostic equation for Turbulent Kinetic Energy (TKE or E) combined with a diagnostic length scale:

$$K = l_{turb}\sqrt{E} \quad (2)$$

Different TKE- l schemes use rather different rules to prescribe the length scale l_{turb} in terms of local and/or nonlocal stability measures: e.g. based on a parcel method in MESO-NH (Bougeault and Lacarrère 1989) or based on the local Ri in ECHAM4 (Roeckner *et al.* 1996). The Louis (1979) closure uses

$$K = l_{turb}^2 \left| \frac{\partial\bar{U}}{\partial z} \right| \quad (3)$$

with l_{turb} depending on the Richardson number, chosen such that near the surface the scheme matches to surface flux profile relations. The K -profile method (Troen and Mahrt 1986) uses prescribed, approximately quadratic profiles, from

the surface to the top of the convective boundary layer. In such a scheme, the entrainment flux at the boundary layer top is often prescribed.

ECMWF and METO use a K -profile method with prescribed entrainment rate, and ARPEGE the 2nd order Mellor and Yamada (1974) scheme based on diagnostic (instead of prognostic) TKE. For stable conditions ECMWF uses the Louis (1979) closure. The other models use a TKE- l scheme, but with rather different formulations of the length scale.

The profiles of the eddy diffusivity for heat K_h at 17.30 UTC are shown in Fig. 7. In the cloud layer ARPEGE and ECHAM4 have profiles that are spatially incoherent with spikes up to unrealistically high values of 500-1000 $\text{m}^2 \text{s}^{-1}$ (Fig. 7a). All other models have rather similar “quadratic” shapes for K_h , but with rather different maximum values ranging from 100 to 300 $\text{m}^2 \text{s}^{-1}$. Usually this maximum is estimated to be order $0.1 h w_*$ (Holtslag and Moeng 1991), with h the dry convective boundary layer height and w_* the convective velocity scale. In our case this gives an estimate of K_h of about 150 $\text{m}^2 \text{s}^{-1}$. It should be noted that in practice there is not such a big difference between a value of 100 and a value of 300 $\text{m}^2 \text{s}^{-1}$, since the subcloud boundary layer will remain well-mixed in both cases. Also nonlocal transport terms might play a role: Stevens (2000) showed that the value of K_h and the nonlocal transport term are related, producing in certain regimes realistic thermodynamic lapse rates. Except METO, none of the SCMs considered here have explicit nonlocal transport terms, and consequently they retain a slightly unstable lapse rate until the base of the entrainment layer at the top of the dry convective boundary layer.

(b) *Moist turbulent mixing*

ECHAM4, RACMO, ARPEGE and MESO-NH have turbulence schemes that represent cloud condensation effects in the computation of the buoyancy fluxes and atmospheric stability. The buoyancy flux can be computed from the fluxes of total water and liquid water potential temperature by:

$$\rho c_p \overline{w'\theta'_v}|_{u,s} = \alpha_{u,s} \rho c_p \overline{w'\theta'_l} + \beta_{u,s} \rho L \overline{w'q'_t}, \quad (4)$$

where α and β [for exact definitions see e.g. Cuijpers and Duynkerke (1993)] are dependent on whether the atmosphere is unsaturated with no cloud water (subscript u) or saturated (subscript s). In dry conditions, $\alpha_u = 1$ and $\beta_u \approx 0.07$. With a latent heat flux of 500 W m^{-2} and a sensible heat flux of 140 W m^{-2} the moisture flux amounts to about 30 % of the buoyancy flux. In the saturated conditions, however, $\alpha_s \approx 0.5$ and $\beta_s \approx 0.4$, which, in this case, means that the moisture flux dominates the buoyancy flux for saturated conditions. The vertical stability is computed from the gradients of q_t and θ_l in a similar way. In partly cloudy conditions, the buoyancy flux is obtained by a linear interpolation in cloud fraction a of the dry and moist contributions:

$$\rho c_p \overline{w'\theta'_v} = (1 - a) \rho c_p \overline{w'\theta'_v}|_u + a \rho c_p \overline{w'\theta'_v}|_s \quad (5)$$

For skewed motions Eq. (5) can be extended to include the non-Gaussian part (Cuijpers and Bechtold 1995). This is done in MESO-NH and will be done in next version of ARPEGE. This however may induce overlap with the convection scheme (“double counting”).

In addition, these models (except ARPEGE) use mixing in moist conserved quantities (e.g. in q_t and θ_l) or add separate mixing of cloud liquid water.

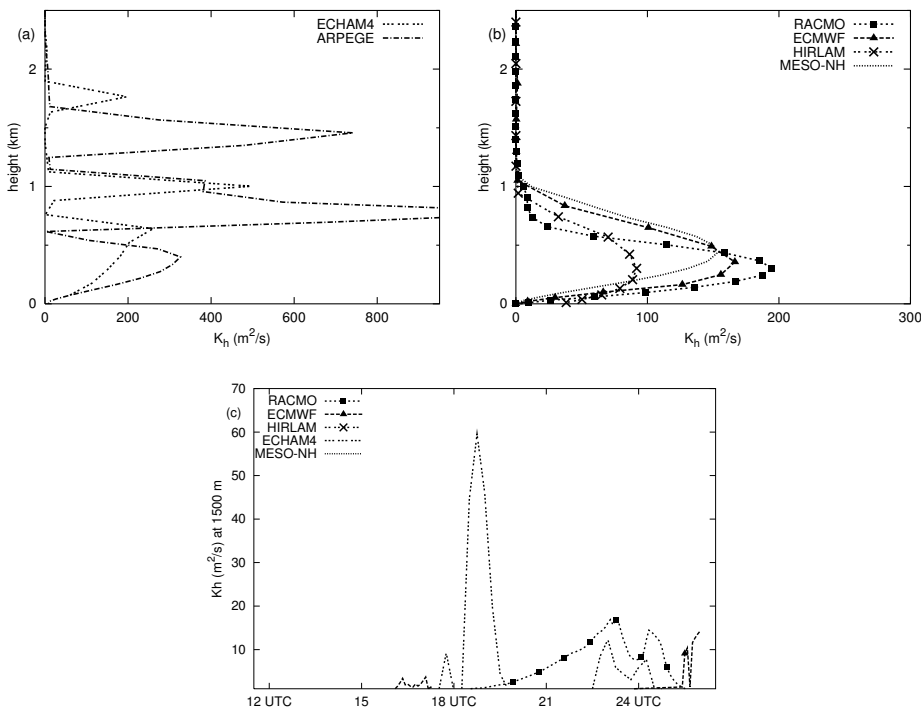


Figure 7. Profiles of K_h at 17.30 UTC for a) ECHAM4 and ARPEGE, b) RACMO, ECMWF, HIRLAM, and MESO-NH, and c) timeseries of K_h in the cloud layer at 1500 m (all in m²s⁻¹)

Although the use of diffusion for cloud liquid water might be questioned, the procedure of mixing liquid and water vapor separately can lead to realistic fluxes of conserved variables – diffusion is a linear operator – in cloudy boundary layers (for a discussion on this subject see e.g. Lenderink and van Meijgaard 2001).

Because the formulation of buoyancy flux given by Eq. (5) is strongly dependent on the cloud fraction, small changes in cloud fraction have a large impact on the atmospheric stability and the buoyancy flux. The dependency in moist turbulence scheme may give rise to instability (in ARPEGE and ECHAM4) and cloud regime transitions from Cu to more stratiform clouds (in RACMO), or vice-versa. In ECHAM4 the instability is related to the limit behavior of the Louis (1979) stability functions for small wind shear in combination with a moist formulation for stability (Lenderink and van Meijgaard 2001; Lenderink *et al.* 2000). In that case, small local variations in cloud fraction strongly impact on the computed atmospheric stability, and therefore on the length scale and turbulent mixing. The turbulent fluxes again feed back onto cloud fraction by changing humidity and temperature profiles. Potentially, this is a very strong destabilizing feedback loop. The instability in ECHAM4 is visible from the timeseries and profiles of K_h in the cloud layer in Fig. 7. In RACMO a similar feedback gives rise to increasing cloud cover with time. More active mixing in the cloud layer tends to straighten the profiles, giving rise to a shallow but well mixed boundary layer representative for stratiform clouds. This positive feedback is e.g. visible in the time series of K_h in the cloud layer (Fig. 7). In stratiform clouds long wave

cooling is an important source of turbulence, but in the present case setup it is neglected. Taking longwave cooling into account, we might expect this feedback to have a stronger effect, resulting in still higher cloud fractions.

(c) *Convection*

All models except ARPEGE run with an explicit parameterization of convective transports in the cloud. HIRLAM uses an adapted version of the Kuo (1974) scheme; all other models use a bulk mass flux approach: RACMO, ECHAM4, ECMWF based on Tiedtke (1989); MESO-NH based on Kain and Fritsch (1990) and in METO based on Gregory and Rowntree (1990). None of the models explicitly switch off turbulent diffusion when the convection scheme is active, so convective transports and turbulent diffusion may act simultaneously in the cloud layer.

In the following analysis we will concentrate on the mass flux closures, mainly because most recent developments in parameterizations of convection have been achieved in these type of schemes. The bulk mass flux approach computes the convective fluxes from

$$\overline{w'\phi'}_{conv} = M(\phi^{up} - \phi) \quad (6)$$

with the equation for the cloud updraft ϕ^{up}

$$\frac{\partial \phi^{up}}{\partial z} = \epsilon(\phi - \phi^{up}) \quad (7)$$

and the mass flux M

$$\frac{\partial M}{\partial z} = (\epsilon - \delta)M \quad (8)$$

Here, ϵ and δ govern the amount of updraft mass due to entrainment and detrainment, respectively. Mass flux schemes mainly differ in how the values at cloud base, and the fractional entrainment and detrainment coefficients, ϵ and δ , are prescribed. In the inversion, the updraft becomes negatively buoyant, and above that zero-buoyancy level the mass flux detrains massively.

In Fig. 8 we plotted the flux produced by the mass flux scheme [as defined by Eq. (6)] for θ_l and q_t . These fluxes represent a warming and drying near cloud base, and a moistening and cooling close to the inversion. In ECHAM4 and ECMWF this effect is very strong. To analyze this behavior we focus first on the mass flux M in Fig. 8c. In the cloud layer, the mass flux in two models (ECMWF and ECHAM4) is constant with height, with massive detrainment in a shallow layer in the inversion. In ECHAM4 it is assumed that 80 % of the detrainment takes place in the first layer above the zero buoyancy level and 20 % in the next level. At this high vertical resolution this causes an extremely rapid detrainment. In MESO-NH the mass flux above cloud base first strongly increases, followed by a rapid decrease. RACMO has a gradual decrease in the mass flux fixed by the entrainment and detrainment coefficients in Siebesma and Holtslag (1996).

It should be noted that all model results have linear profiles of the fluxes of total water and liquid water potential temperature from the surface to cloud base. This represent transport by the organized flow in the subcloud layer connected to the cumulus cloud, drawing moisture and heat from the subcloud layer. This is part of the closure assumption used in the models. The massflux M is not used in the subcloud layer, and its shape in the subcloud layer is therefore irrelevant.

In general, the difference between the updraft and the mean field (not shown) increases with height above cloud base. We illustrate this for moisture by writing

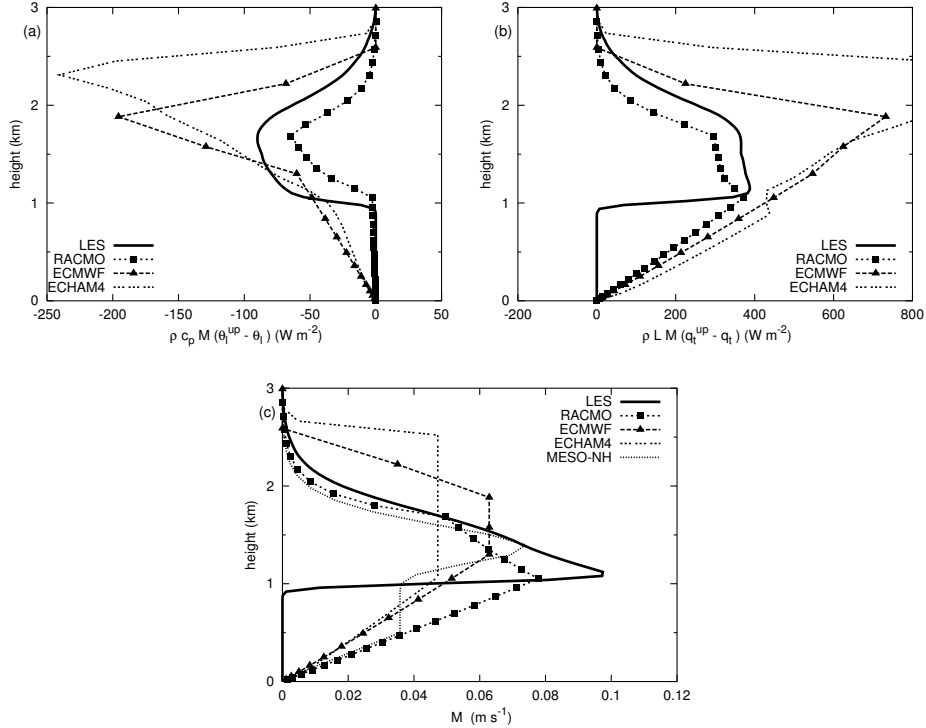


Figure 8. Fluxes of a) θ_t and b) q_t from the mass flux scheme (in W m^{-2}), and c) the mass flux M (m s^{-1})

Eq. (7) as

$$\frac{\partial \Delta q}{\partial z} + \epsilon \Delta q = \Gamma_q, \quad (9)$$

with $\Delta q \equiv q^{up} - q$ and $\Gamma_q \equiv -\frac{\partial q}{\partial z}$. If we assume Γ_q and ϵ constant, just for sake of the argument, this equation can be solved easily (see also Eq. A3 in Siebesma and Holtslag 1996)

$$\Delta q = \frac{\Gamma_q}{\epsilon} + \left(\Delta q_{base} - \frac{\Gamma_q}{\epsilon} \right) e^{-\epsilon(z - z_{base})} \quad (10)$$

with Δq_{base} is Δq at cloud base, and z_{base} the cloud base height. The first term is the asymptotic behavior, and the second term the behavior near cloud base. Taking typical values of $\Delta q_{base} \approx 1 \text{ g kg}^{-1}$, $\Gamma_q \approx 4 \cdot 10^{-3} \text{ g kg}^{-1} \text{ m}^{-1}$ and $\epsilon \approx 2 \cdot 10^{-3}$, the second term is negative, so Δq increases with height above cloud base. Given that in general the mass flux in the SCMs is rather constant or sometimes even increases with height, the flux of the total water increases with height. This reflects that the mass flux scheme takes away moisture from the lowest part of the cloud and deposits this in or close to the inversion. In ECHAM4 and ECMWF this effect is very pronounced (see Fig. 8), being at odds with the LES results and common sense. Hence, the mass flux should decrease with height in order to obtain moisture fluxes that also decrease with height. Similar arguments hold for the flux of liquid water potential temperature.

The increase in the convective flux of total water with height is responsible for the large gradient just above cloud base. In the subcloud layer this gradient does not occur due to the intense mixing by the turbulence scheme. In terms of potential temperature an inversion is created just above the well-mixed subcloud layer. This is clearly visible in the profiles of especially relative humidity in Fig. 5 (ECMWF and ECHAM4). There is a positive feedback because the difference between updraft and mean field increases during this process.

The high moisture content above 2300 m in ECHAM4 and ECMWF are caused by too strong activity of the mass flux scheme, depositing too much moisture in/or just above the inversion. In ECMWF, time series of the mass flux at cloud base revealed that in the first few hours after the onset of the clouds, the mass flux obtained very high values of $0.2 \text{ kg m}^{-2} \text{ s}^{-1}$. This confirms results of Neggers *et al.* (2003), where it was shown for this case that the mass flux closure based on moist static energy convergence strongly overpredicts the cloud base mass flux during the early stages of cloud formation.

All models except HIRLAM trigger convection at about the same time, mainly due to the dominance of the strong surface forcing. However, simulations of the diurnal cycle of Stratocumulus clouds showed that some of the SCMs did also trigger the mass flux scheme in that case, which causes a significant reduction of the cloud cover (Duynkerke *et al.* 2004). Moreover, results shown in Jakob and Siebesma (2003) showed that the triggering function is extremely important in AGCM simulations of ECMWF.

In HIRLAM a switch turns convection smoothly off when the horizontal grid spacing gets finer. This switch is mainly developed with deep convection in mind, but acts for shallow convection also. The results presented here are for a horizontal resolution of 4 km, which is the typical resolution the HIRLAM aims at in the near future. Results at a resolution of 20 km (not shown) are better with much deeper clouds, extending to 2500 m during the mid afternoon. But also in this simulation a rather thick, low-level cloud develops at the end of the day after 23 UTC.

(d) *Interaction of turbulence and convection*

The interaction between the convection scheme and the turbulence scheme plays an important role. Both the turbulence and the mass flux scheme determine how the profiles of temperature and humidity evolve. The resulting profiles, in particular near cloud base, again influence mass flux activity and/or turbulent activity, potentially giving rise to strong feedback loops.

In some models, the role of the turbulence scheme is crucial to prevent unrealistically strong drying of the lower part of the cloud layer due to the mass flux scheme. However, the inversion near cloud base caused by the mass flux scheme may limit turbulent transports. In this case a run-away process may occur. Dry turbulence schemes are slightly more susceptible to this feedback, but it may also occur in moist turbulence schemes. In ECHAM4, the stability functions in terms of the local Ri number, and the limit behavior for small wind shear (Lenderink and van Meijgaard 2001) are responsible for a cessation of turbulent transports across cloud base.

On the other hand, a feedback between the cloud base closure of the mass flux scheme and the turbulence scheme might lead to a reduction of convective activity. This type of feedback may occur with closures based on the assumption of subcloud equilibrium, or more precisely, based on subcloud convergence of

moisture (ECHAM4 and RACMO) or moist static energy (ECMWF). In that case, the mass flux at subcloud is adjusted so that the total moisture (or moist static energy) content of the subcloud layer remains constant:

$$M_{base} = \frac{\overline{w'q'_t}|_s - \overline{w'q'_t}|_{base}}{(q^{up} - q)_{base}} \quad (11)$$

with $\overline{w'q'_t}|_s$ the surface latent heat flux and $\overline{w'q'_t}|_{base}$ the moisture flux through cloud base generated in the turbulence scheme. In this closure the following feedback may occur. If the stability at cloud base weakens, the turbulence fluxes at cloud base will increase. In effect, the closure will reduce the mass flux activity. This process will erode the inversion at cloud base further (due to combined effects of more active diffusion and less mass flux activity). Schemes with moist turbulence schemes are more susceptible to this feedback (e.g. in RACMO). Obviously, this feedback is strongly dependent on the type of closure; for example, it does not occur with closures based on the subcloud turbulent velocity scale (Grant 2001), such as e.g. used in METO.

Since mass flux schemes are basically advection schemes, the way the advection operator is implemented plays an important role. Many of the present-day operational mass flux schemes use implementations that are close to upwind differencing (Tiedtke 1989). They introduce considerable amounts of numerical diffusion (with K order $M \Delta z/2 \approx 1 - 10 \text{ m}^2 \text{ s}^{-1}$ with Δz the grid spacing). In fact, using a non-diffusive central differencing in ECMWF, large gradients at cloud base occurred. Since at high resolution numerical diffusion becomes insignificant, these models tend to become more unstable with increased vertical resolution. In combination with turbulence schemes based on local stability measures (like e.g. the Richardson number) this may give rise to high levels of noise.

(e) cloud schemes

There is a large spread in how models treat cloud fraction, cloud liquid water, and evaporation and condensation. The range spans from statistical schemes, which diagnose cloud liquid water and cloud fraction based on mean values of q_t and θ_t and estimates of their subgrid variability (in MESO-NH and ARPEGE) to process-based schemes with prognostic equations for both cloud liquid water and cloud fraction (ECMWF). Other models combine a diagnostic cloud cover, based on relative humidity (HIRLAM, ECHAM4) or total water (RACMO), with a prognostic equation for cloud condensate based on Sundqvist *et al.* (1989). Due to this variety in cloud schemes used, it is hard to draw general conclusion from the results. In addition, the fact that most models drift away from realistic temperature and humidity profiles rather quickly (as is shown in Fig. 5) complicates the analysis. A perfect model approach in which cloud schemes are fed with realistic mean profiles would be more revealing, but this approach was not exercised here. An example of such an approach is discussed in Siebesma *et al.* (2003).

One rather general conclusion one might draw from the results is that in the prognostic schemes cloud fraction and cloud liquid water are (often) strongly tied to the convective activity. For example, in these models the detrainment of liquid water by the mass flux scheme is used as a source term for the liquid water, given

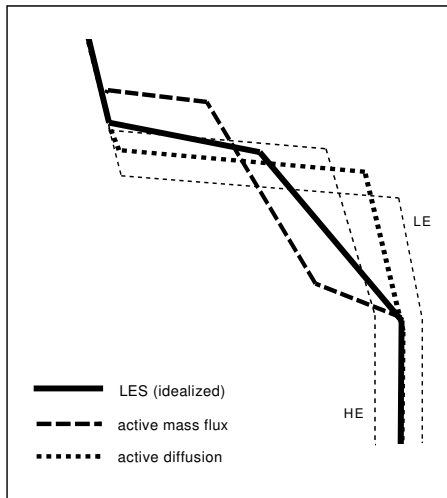


Figure 9. Typical idealized profiles of moisture resulting from models characterized by (too) strong turbulent mixing, and (too) strong mass flux activity. The thick solid line represents the idealized profile from LES (reference). The thin lines labelled with HE and LE denote an “active diffusion” case with high entrainment rate and low entrainment rate at cloud top, respectively. The “active mass flux” case responds in a similar way to cloud top entrainment.

by:

$$\left(\frac{\partial q_l}{\partial t}\right)_{detr} = q_l^{up} \max(0, -\frac{\partial M}{\partial z}) \quad (12)$$

In several models (ECHAM4, RACMO, and ECMWF) this leads to a peak in cloud liquid water content close to the inversion where massive detrainment takes place. In ECMWF a similar term is also used in the prognostic equation for the cloud fraction leading to high cloud fractions in the inversion. These high values of the cloud related parameters occur despite the relatively low humidity, which does not appear to be a very realistic feature (for more on this issue see also Teixeira 2001).

5. PROGRESS

(a) *Synthesis of previous results*

The activity of both mass flux and turbulence schemes, and their relative strengths, are major issues. To summarize, we plotted in Fig. 9 two different profiles of total water corresponding to two typical cases of the SCM results. The “active diffusion” case represents a model with strong diffusive activity (and corresponding weak or normal mass flux activity). In the cloud layer profiles are too close to the moist adiabat (too straight). Cloud fraction is accordingly too high. The turbulence scheme tends to produce a relatively low inversion with a sharp gradient. The “active mass flux” case corresponds to a model with too strong mass flux activity. In this model too much moisture is taken out of the lower part of the cloud and deposited near the inversion. In this case cloud fraction tends to peak near the inversion.

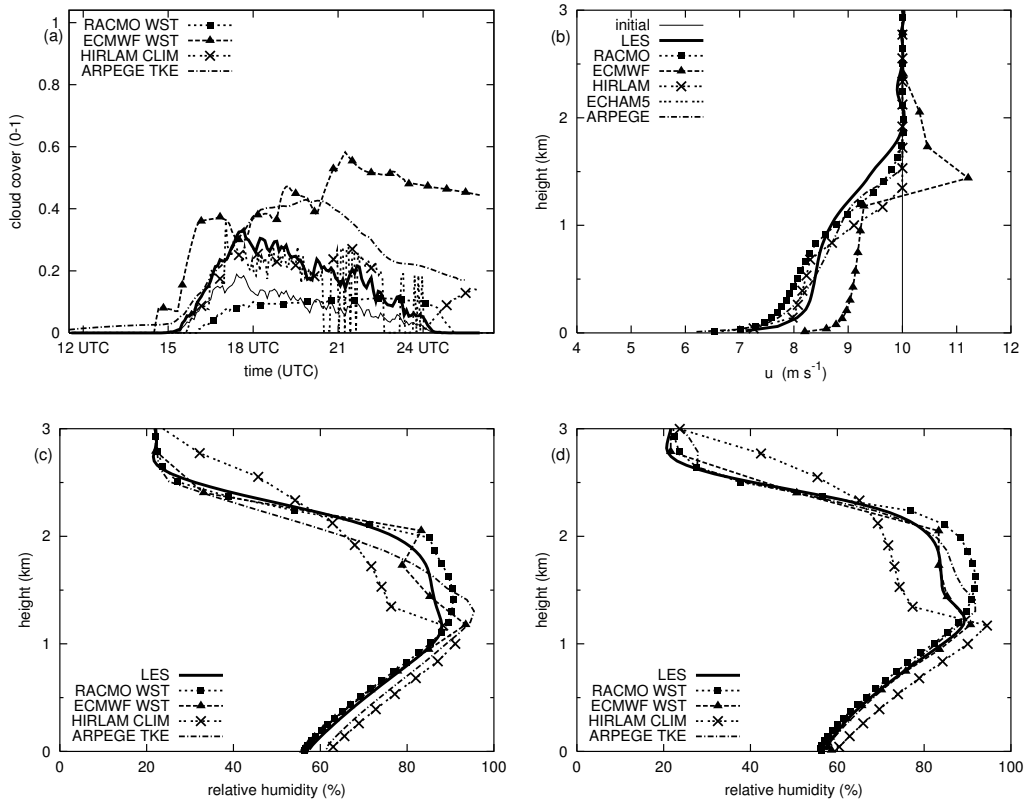


Figure 10. Time series of cloud cover (a), and profiles of wind (b), and relative humidity at 21.30 (c) and 1.30 UTC (d) in the updated models.

(b) Results of updated models

Based on the findings described above, many participants updated their models with new physics schemes and/or modified their present schemes. Results of some successful updates are shortly described below. It is not our goal to describe and analyze these changes extensively. Merely, we would like to illustrate which type of modifications may lead to improved results. Significant improvements were obtained in four models which are referenced by ECMWF-WST, RACMO-WST, ARPEGE-TKE, and HIRLAM-CLIM. Though there might have been some tuning for the present case in these models, the models are certainly not strongly tuned and the parameters used (e.g. for the w_* closure) are close to what has been reported in literature.

ECMWF-WST uses a new closure of the cloud base mass flux based on the convective velocity scale (Grant 2001)

$$M_{base} = aw_* \quad (13)$$

with $a = 0.03$. The closure based on subcloud moist static energy convergence employed in the reference version gave unrealistically high values of the cloud base mass flux in the early hours of cloud formation. This is prevented by using Eq. (13). Also the boundary layer scheme for convective conditions was replaced

(Siebesma and Teixeira 2000) and the updraft properties at cloud base were computed from a new parcel method (Jakob and Siebesma 2003).

RACMO-WST also employs the convective velocity scale closure by Eq. (13), but with slightly higher value $a = 0.04$. The main reason for this change is that the used moisture convergence closure gave rise to a regime transition to higher cloud fractions at the end of the simulation period. In addition, mixing of momentum in the mass flux scheme was turned off, but at the same time vertical diffusion was added by

$$K_{mf} = l_{mf}M \quad (14)$$

with $l_{mf} = 100$ m. The length scale l_{mf} chosen so that about 20-30 % of the total flux of q_t and θ_l in the cloud is due to diffusion and the other part due to the mass flux as supported by LES results in Siebesma *et al.* (2003). One may consider this additional diffusion as representing mixing by the smaller eddies in the cloud; it is done for heat, moisture and momentum.

To improve the numerical stability in ARPEGE-TKE the diagnostic turbulence closure was replaced by a prognostic TKE- l scheme with the Bougeault and Lacarrère (1989) “parcel” length scale. The moist turbulence scheme has been extended with mixing in moist conserved variables, and a nonlocal term (skewed) is added to Eq. (5). A mass flux scheme has been added based on the ideas of Kain and Fritsch (1990) and described in Bechtold *et al.* (2001). Chaboureau and Bechtold (2002) and Lopez (2002) describe the new cloud and condensation scheme.

Finally, in the HIRLAM-CLIM the main change was a replacement of the cloud and convection scheme STRACO by a package developed by the SMHI Rossby climate modeling center consisting of the Kain and Fritsch (1990) convection scheme and Rasch and Kristjánsson (1998) cloud/condensation scheme (Uden *et al.* 2002).

Results of these updated schemes are shown in Fig. 10. The time series of the cloud cover show lower, more realistic values below 40 % in the models, except in ECMWF-WST. The latter is caused by the prognostic cloud scheme in which cloud cover is too strongly tied to the (massive) detrainment of the mass flux scheme. The thermodynamical profiles are significantly improved in all models as can be seen from the relative humidity profiles, though HIRLAM-CLIM shows the footprint of too strong mass flux activity. The wind profiles in RACMO-WST are vastly improved due to deactivation of momentum transport by the mass flux scheme and the inclusion of additional diffusive momentum transport. In HIRLAM-CLIM there is a trace of numerical instability left.

To illustrate both the activity of the diffusion and the mass flux scheme, we plotted K_h and M at 21.30 UTC in Fig. 11. The mass fluxes are of the same order of magnitude, but the different models have rather different shapes; ranging from constant with height (ECMWF-WST), uniformly decreasing with height (RACMO-WST), to first increasing and then decreasing with height in the two Kain and Fritsch (1990) based models (ARPEGE-TKE and HIRLAM-CLIM). All models have similar quadratic shape profiles of K_h in the subcloud layer with small values in the cloud layer.

Finally, in ECHAM (results not shown) the change of the cloud cover scheme from a relative humidity based scheme (Sundqvist *et al.* 1989) to a statistical

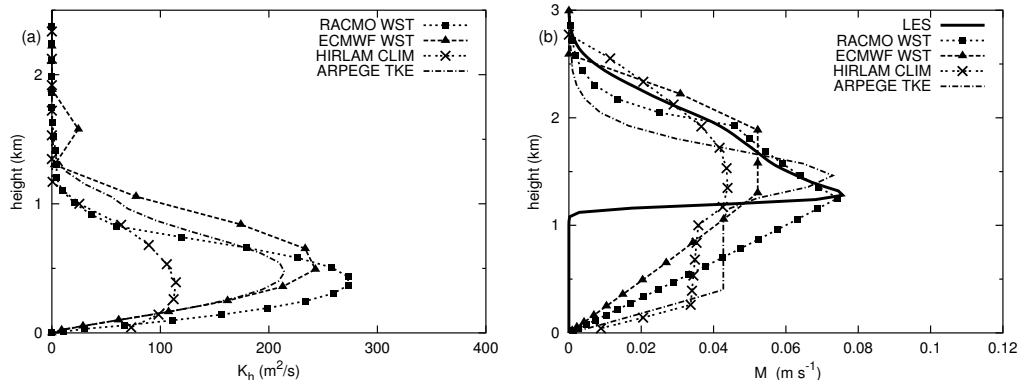


Figure 11. Eddy diffusivity and mass flux profiles at 21.30 UTC in the updated models.

cloud cover scheme (Tompkins 2002) vastly improved the onset of cloud formation. However, the convective and turbulent transport still caused a significant moist bias close to the inversion, causing high cloud amounts.

(c) Resolution dependency

The results of most models depend strongly on vertical resolution. To illustrate typical model resolution dependencies we present results of ECHAM4, METO, RACMO-WST, ARPEGE-TKE at R_{19} and R_{40} resolution in Fig. 12. In ECHAM4, results of the high resolution are much more contaminated by gridpoint noise. The results on R_{19} are reasonable, but the R_{40} results are unacceptable due to instabilities related to the turbulence scheme. In RACMO the results on R_{19} are characterized by a more shallow and moist cloud layer. This is related to the fact that the layer with massive detrainment at cloud top is diagnosed as the whole layer immediately below the first level where the cloud updraft is negatively buoyant. It does not take into account that part of this layer may be in the active buoyant cloud where there should be no massive detrainment. In particular, on low resolution too much moisture is therefore deposited in the active cloud. Results of RACMO-WST obtained with a 50 m grid spacing are almost identical to the R_{40} results, showing that this effect becomes insignificant at R_{40} resolution.

The results of METO and ARPEGE-TKE show rather large sensitivities to vertical resolution. The low resolution results are considerable more moist in the subcloud layer (1-2 g kg⁻¹), and gradients at cloud base are (much) larger. The latter reflects the weak activity of the turbulence scheme across cloud base (unable to moisten the lower part of the cloud layer sufficiently) and/or the strong activity of the mass flux scheme. In METO the signature of the simulation changes from a typical “active diffusion case” at R_{40} to a “active mass flux case” at R_{19} (see Fig. 9). In ARPEGE this effect is also visible, but less pronounced.

It is noted that METO and ECHAM4 perform (somewhat) better on R_{19} resolution. In ECHAM4 the amount of gridpoint noise is significantly lower on R_{19} compared to the high resolution results. In METO the properties of the subcloud layer are close to the LES, but the cloud layer shows in imprint of a too active

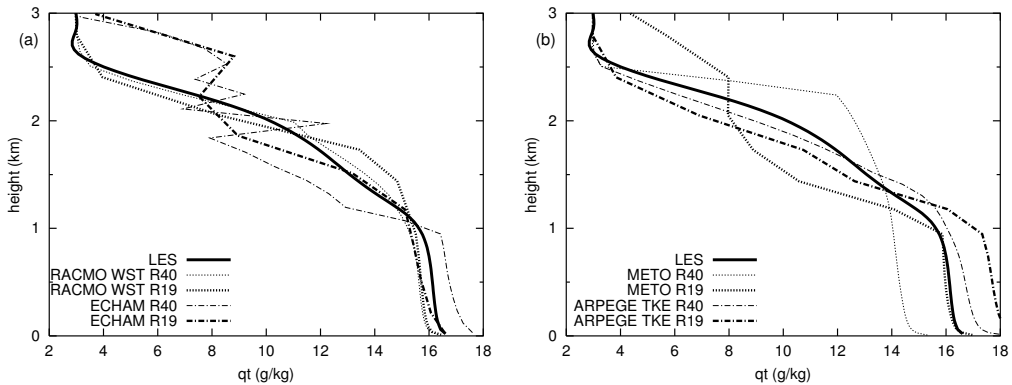


Figure 12. Results of the SCM on two different vertical resolution. Shown are profiles of total water at 21.30 UTC.

mass flux scheme. Results of METO on R_{19} are rather close to the results of the resolution the model is run operationally.

(d) *Unified approaches*

Considering the ad-hoc way turbulent diffusion schemes and convection schemes are coupled, it appears advantageous to use unified approaches to represent fluxes in cloud and subcloud layer. Therefore, as a bonus, results of three research models based on such an approach are presented.

Two models, MESO-DIF [described in Sanchez and Cuxart (2003)] and CHEIN-DIF [described in Cheinet and Teixeira (2003)], employ a unified approach based on diffusion using a moist TKE- l closure. Results in Fig. 13 of these show a reasonable skill to predict the temperature and moisture profile, in particular when compared to the results of the operational SCMs (see Fig. 5). On the downside, however, the results are characterized by a rather high level of intermittency in the cloud layer related to the interaction of the moist turbulence scheme with the cloud condensation physics (as discussed in Section 4b). Also these models tend to create a too sharp inversion, reflecting that a local diffusion scheme is not able to represent the overshoots of the strongest updrafts in the inversion.

CHEIN-MF uses a multi-parcel mass flux approach (Cheinet 2003). As shown in Fig. 13, the temperature and humidity profiles predicted by CHEIN-MF are very close to the LES results, both in the cloud layer and in the sub-cloud layer. The fact that the same entraining plume model is used for the unsaturated and the saturated updrafts is thought to explain the consistent treatment of the sub-cloud and cloud layer mixing. Timing of the convective activity is very good (see the liquid water path in Fig 13c). Since this model is purely diagnostic with respect to the turbulence variables, this suggests that the cloud layer adjusts very rapidly to the surface forcing in our case. Also, the model results turned out to be (much) less sensitive to vertical resolution compared to bulk mass-flux approaches (Cheinet 2003).

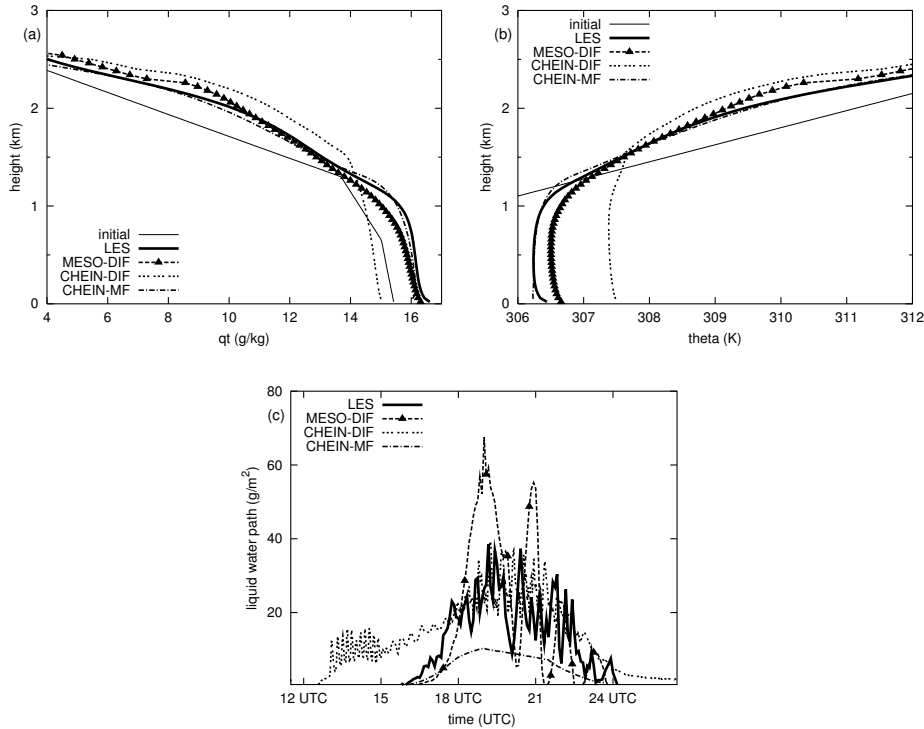


Figure 13. Results of the models based on a unified approach. Shown are the profiles of a) q_t (g kg^{-1}) and b) θ (K) at 2130 UTC and c) the time series of the cloud liquid water path (g m^{-2}).

6. DISCUSSION

An intercomparison of the diurnal cycle of cumulus convection in different SCMs derived from (semi-) operational models is presented. The SCM results revealed several deficiencies. In general, results are characterized by: too large values of cloud liquid water and cloud cover, strong intermittent behavior, and unrealistic profiles of temperature and humidity (and wind) in the cloud layer.

The results are analyzed in terms of the behavior of the different parameterization schemes involved: the turbulence scheme, the cumulus convection scheme, and the clouds and condensation scheme. The different models have different causes for their deficiencies. The main causes are (not applying all to one model):

- Too strong activity of the turbulence scheme in the cloud layer, giving rise to too strongly mixed, and in most cases too shallow and too moist boundary layers.
- Too strong activity of the mass flux scheme causing a too dry (warm) lower part of the cloud, and a too moist (cold) upper part. Often a (strong) temperature inversion at cloud base results, prohibiting any further turbulent transport across cloud base.
- Unrealistic feedback loops between mass flux activity and (subcloud) turbulence, in particular related to the mass flux closure.
- Unrealistic transport of momentum in the mass flux scheme

- Strong intermittency mainly caused by the interaction of the (moist) turbulence scheme with the cloud scheme and the convection scheme
- Too strong dependency of the cloud/condensation scheme on the (massive) detrainment by the mass flux scheme.

In general, the SCM results could be divided into two different classes. In one class, turbulent activity was too strong and in the other class the mass flux activity was too strong. Typical, idealized profiles obtained in these classes are shown in Fig. 9. Paradoxically, in both classes too high values of cloud cover and liquid water content occur: in the first class being a realistic consequence of the shallow, moist boundary layer, in the second class mainly caused by the (unrealistically) strong dependency of cloud liquid water and/or cloud fraction on the detrainment from the mass flux scheme. In this respect the closure assumption of the mass flux scheme plays a crucial role; see also Neggers *et al.* (2003) for the impact of different closure assumptions for the present case.

Due to the large surface forcing, the triggering of convection is not a major issue here. The initialization of convection is determined by the so-called “trigger-function” which essentially is an explicit rule determining the on and off switching of convection; for example, using the buoyancy of a parcel originating from the surface at the lifting condensation level. However, some of the schemes presented here also trigger convection in a Stratocumulus case (Duykerke *et al.* 2004), showing that in general the trigger function is very important.

The dependency of the results on vertical resolution is a major issue. Results of the models do not necessarily converge or become better at high resolution. Models tend to suffer from numerical instabilities at higher resolution originating from the turbulence scheme and its interaction with the cloud and condensation scheme, and the convection scheme. In addition, the reduced numerical diffusion in (advective) mass flux schemes at high resolution may degrade the results. Trivially, numerical unstable models do not produce converged results with higher resolution. Also hidden resolution dependencies in the code, e.g. in the mass flux scheme, may come into play. Convergence for RACMO-WST at a resolution of 200 m in the cloud layer has been established. But for the other operational models such convergence could not be proved.

Based on these findings, several SCMs have been updated with new physics packages and/or their present packages have been revised. These new model perform significantly better on this case, though there are some remaining deficiencies. All updated models use a bulk mass flux approach combined with diffusion in the subcloud layer. For this combination, the following specific recommendations are made:

- use a turbulence scheme based (predominantly) on nonlocal stability characteristic (e.g., Bougeault and Lacarrère 1989; Lenderink and Holtslag 2004).
- use a mass flux closure based on the convective velocity scale of the subcloud layer (e.g., Grant 2001).
- use either local diffusion for transport of momentum in the cloud layer, or a mass flux approach with weak nonlocal characteristics; that is, with updraft properties which relax strongly to environmental profiles [see also Brown (1999) for more on this issue]
- use a statistically based cloud scheme, or a prognostic scheme with a weaker (than presently used in many models) dependency on the massive detrainment by the mass flux scheme.

TABLE A.1. MODEL DETAILS

Scientists	Model ^α	Diffusion ^β	Convection ^γ	Cloud ^δ
Marquet	ARPEGE[-TKE] ¹	TKEd [TKE] / d [m]	no [KF]	Dc / DI [PI]
Siebesma	ECMWF[-WST]	PRO / d	T	Pc / PI
Mueller (Chlond)	ECHAM4 ²	TKE / m	T	Dc / PI
Lenderink	RACMO[-WST] ³	TKE / m	T	Dc / PI
Irons	METO	PRO / m	GR	Dc / DI
Soares (Miranda)	MESO-NH ⁴	TKE / m	KF	Dc / DI
Olmeda/Calvo	HIRLAM ⁵	TKE / d	KUO	Dc / PI
Jones	HIRLAM-CLIM ⁵	TKE / d	KF	Dc / PI
Sanchez (Cuxart)	MESO-DIF	TKE / m	no	Dc / DI
Cheinet	CHEIN-DIF	TKE /m	no	Dc / DI
Cheinet	CHEIN-MF	no	MulMF	Dc / DI

[..] updated model versions

^α Main model reference: ¹Gibelin and Déqué (2003), ²Roeckner *et al.* (1996), ³Lenderink *et al.* (2000), ⁴Lafore *et al.* (1998), ⁵Uden *et al.* (2002)

^β Dry (d) stands mixing in dry variables only;(m) stand for mixing in moist variables and/or computation stability in moist variables. TKE stands for a prognostic TKE, TKEd for diagnostic TKE, PRO for a K-profile method

^γ KF stand for Kain and Fritsch (1990); T stands for Tiedtke (1989), KUO for Kuo (1974); GR for Gregory and Rowntree (1990); and MulMF for Multiple Massflux (Cheinet 2003)

^δ Pc stand for prognostic cloud cover, Dc diagnostic cloud cover, PI prognostic cloud liquid water, and DI diagnostic cloud liquid water.

It should be noted that we do not argue that with other (type of) schemes realistic results cannot be obtained; we argue that SCMs that satisfy these points perform reasonably well in the present case.

Summarizing, the paper shows that the present state of cloud modeling has three major sources of errors which are related to: i) our understanding of the basic physical processes, ii) our understanding of how to couple what we regard as distinct processes, and iii) the numerical implementation of these processes on a grid. In particular, the last two points are considered to be most important. With respect to the second point, multiple mass flux approaches, such as e.g. proposed by Cheinet (2003) and Neggers *et al.* (2002), are a promising way of achieving a (numerically stable) consistent treatment of subcloud layer turbulence and cloud mixing.

ACKNOWLEDGEMENTS

This work benefited greatly from discussions during several EUROCS workshops. In particular, we would like to thank Joan Cuxart, Andreas Chlond, Pedro Miranda, Bjorn Stevens and an anonymous reviewer for their comments on earlier versions of this paper. This study has been made with financial support of the European Union (Contract number EVK2-CT-1999-00051).

APPENDIX A

Appendix A Model description

The physics packages of the (semi-) operational model are summarized in Table 1. Below follows some more detailed information.

ARPEGE employs a 2nd order Mellor and Yamada (1974) turbulence closure with diagnostic value of TKE. Mixing is done in dry static energy and water vapor only, though the scheme uses a moist formulation for stability (Bougeault

1982). For shallow convection the mass flux scheme is inactivated. A statistical cloud scheme (Ricard and Royer 1993) with diagnostic cloud liquid water and cloud fraction is used.

ECHAM4 (Roeckner *et al.* 1996) uses a moist turbulence scheme based on prognostic TKE, with the length scale formulation based on Louis (1979). The convection scheme is the bulk mass flux scheme by Tiedtke (1989). The Sundqvist *et al.* (1989) scheme is used for cloud condensation and evaporation. Cloud fraction is based on relative humidity.

RACMO is based on ECHAM4 physics. The length scale in ECHAM4 turbulence scheme has been replaced in order to improve the behavior for (moist) convective conditions as discussed in Lenderink and Holtslag (2004). The cloud fraction is computed by a simple statistical scheme with a link between mass flux activity and the variance of total water used in the cloud scheme (Lenderink and Siebesma 2000). RACMO uses the Tiedtke (1989) mass flux scheme, but with modified (increased) entrainment and detrainment coefficients for shallow convection (Siebesma and Holtslag 1996).

ECMWF uses the Louis (1979) scheme for stable and a K-profile method (Troen and Mahrt 1986) for unstable conditions with a prescribed top entrainment rate. The scheme mixes “dry” variables only (water vapor and dry static energy) and is based on dry formulation for stability. The convection scheme is the Tiedtke (1989) mass flux scheme. ECMWF uses a fully prognostic cloud scheme with prognostic equations for both cloud fraction and cloud condensate (Tiedtke 1993).

HIRLAM uses a “dry” TKE- l scheme with the Bougeault and Lacarrère (1989) parcel length scale formulation (Cuxart *et al.* 2000). The convection and cloud scheme is STRACO (Soft Transition Condensation), which combines a modified Kuo (1974) convection scheme with clouds and condensation based on Sundqvist *et al.* (1989). A switch has been introduced to smoothly turn off convection in the full 3D model for horizontal resolutions below 10km. The present SCM simulations used a 4 km resolution which means that the convective tendencies are significantly reduced.

METO uses a K-profile method combined with prescribed entrainment rates to compute turbulent fluxes. It uses a nonlocal transport term in convective conditions (Holtslag and Boville 1993). It mixes conserved variables and is based on a moist formulation of stability. The Gregory and Rowntree (1990) convection scheme is used, together with a closure based on w_* (Grant 2001). The entrainment rates are as Grant and Brown (1999). The cloud scheme is diagnostic based on relative humidity.

MESO-NH uses a moist turbulence scheme (Cuxart *et al.* 2000) based on the Bougeault and Lacarrère (1989) length scale. The mass flux used is the Kain and Fritsch (1990) mass flux scheme. It uses a statistical cloud scheme based on total water and liquid water potential temperature.

REFERENCES

- | | | |
|---|------|---|
| Bechtold, P., Bazile, E.,
Guichard, F., Mascart, P.
and Richard, E. | 2001 | A Mass flux convection scheme for regional and global models. <i>Quart. J. Roy. Meteor. Soc.</i> , 127 , 869–886 |
| Bougeault, P. | 1982 | Cloud-Ensemble Relations Based on the Gamma Probability Distribution for the Higher-Order Models of the Planetary Boundary Layer. <i>J. Atmos. Sci.</i> , 39 , 2691–2700 |

- Bougeault, P. and Lacarrère, P. 1989 Parameterization of Orography-Induced Turbulence in a Mesobeta-Scale model. *Mon. Wea. Rev.*, **117**, 1872–1890
- Brown, A. R. 1999 Large-Eddy Simulation and Parametrization of the effects of shear on shallow cumulus convection. *Boundary-Layer Meteorology*, **91**, 65–80
- Brown, A. R., Cederwall, R. T., Chlond, A., Duynkerke, P. G., Golaz, J.-C., Khairoutdinov, J. M., Lewellen, D. C., Lock, A. P., Macvean, M. K., Moeng, C.-H., Neggers, R. A. J., Siebesma, A. P. and Stevens, B. 2002 Large-eddy simulation of the diurnal cycle of shallow cumulus convection over land. *Quart. J. Roy. Met. Soc.*, **128(B)**, 1075–1094
- Browning, K. A. 1993 The GEWEX Cloud System Study (GCSS). *Bull. of the Amer. Met. Soc.*, **74**, 387–399
- Chaboureau, J.-P. and Bechtold, P. 2002 A Simple Cloud Parameterization Derived from Cloud Resolving Model Data: Diagnostic and Prognostic Applications. *J. Atmos. Sci.*, **59**, 2362–2372
- Cheinet, S. 2003 A Multiple Mass-Flux Parameterization For the Surface-Generated Convection. Part 2: Cloudy Cores. *Accepted pending minor revisions, JAS*, , 18
- Cheinet, S. and Teixeira, J. 2003 A simple Formulation for the eddy-diffusivity parameterization of cloudy boundary layers. *Geophys. Res. Letters*, **30(18)**, 1930 doi:10.1029/2003GL017377
- Cuijpers, J. W. M. and Bechtold, P. 1995 A Simple Parameterization of Cloud Related Variables for Use in Boundary Layer Models. *J. Atmos. Sci.*, **52**, 2486–2490
- Cuijpers, J. W. M. and Duynkerke, P. G. 1993 Large-eddy simulation of trade-wind cumulus clouds. *J. Atmos. Sci.*, **50**, 3894–3908
- Cuxart, J., Bougeault, P. and Redelsperger, J.-L. 2000 A turbulence scheme allowing for mesoscale and Large-Eddy Simulations. *Quart. J. Roy. Met. Soc.*, **126**, 1–30
- Duynkerke, P. G., de Roode, S. R. and 17 Co-authors 2004 Observations and numerical simulation of the diurnal cycle of the EUROCS stratocumulus case. Submitted to QJRM (this special issue)
- Gibelin, A.-L. and Déqué, M. 2003 Anthropogenic climate change over the Mediterranean region simulation by a global variable resolution model. *Climate Dynamics*, **20**, 327–339
- Grant, A. L. M. 2001 Cloud-base fluxes in the cumulus-capped boundary layer. *Quart. J. Roy. Met. Soc.*, **127**, 407–422
- Grant, A. L. M. and Brown, A. R. 1999 A similarity hypothesis for shallow cumulus transports. *Quart. J. Roy. Met. Soc.*, **125**, 1913–1936
- Gregory, D. and Rowntree, P. R. 1990 A mass flux convection scheme with representation of cloud ensemble characteristics and stability- dependent closure.. *Mon. Wea. Rev.*, **118**, 1483–1506
- Holtslag, A. A. M. and Boville, B. A. 1993 Local versus nonlocal boundary-layer diffusion in a global climate model.. *J. Climate*, **6**, 1825–1842
- Holtslag, A. A. M. and Moeng, C.-H. 1991 Eddy diffusivity and countergradient transport in the convective atmospheric boundary layer. *J. Atmos. Sci.*, **48**, 1690–1698
- Jakob, C. and Siebesma, A. P. 2003 A new subcloud model for mass-flux convection schemes: Influence on triggering, updraft properties and model climate. *Mon. Wea. Rev.*, **131**, 2765–2778
- Kain, J. S. and Fritsch, J. M. 1990 A one-dimensional entraining/detraining plume model and its application in convective parameterization. *J. Atmos. Sci.*, **47**, 2784–2802
- Kuo, H. L. 1974 Further Studies of the Parameterization of the Influence of Cumulus Convection on Large-Scale Flow. *J. Atmos. Sci.*, **31**, 1232–1240

- Lafore, J.-P., Stein, J., Asensio, N., Bougeault, P., Ducrocq, V., Duron, J., Fischer, C., Hereil, P., Marcart, P., Pinty, J.-P., Redelsperger, J.-L., Richard, E. and Vila-Guerau de Arellano, J. 1998 The Meso-NH atmospheric simulation system. Part 1: Adiabatic formulation and control simulations.. *Annales Geophysicae*, **16**, 90–109
- Lenderink, G. and Holtslag, A. A. M. 2004 An Updated Length Scale Formulation for Turbulent Mixing in Clear and Cloudy Boundary Layers. Accepted QJRMS (this special issue)
- Lenderink, G. and van Meijgaard, E. 2001 Impacts of cloud and turbulence schemes on integrated water vapor: Comparison between model predictions and GPS measurements. *Meteor. Atm. Phys.*, **77**, 131–144
- Lenderink, G., van Meijgaard, E. and Holtslag, A. A. M. 2000 Evaluation of the ECHAM4 cloud-turbulence scheme for Stratocumulus. *Meteor. Zeitschrift*, **9**, 41–47
- Lenderink, G. and Siebesma, A. P. 2000 ‘Combining the Massflux Approach with a statistical cloud schemes’. Pp. 66–69 in Proceedings of 14th Symposium on Boundary Layers and Turbulence, Aspen, USA. American Meteorological Society
- Lopez, P. 2002 Implementation and validation of a new prognostic large-scale cloud and precipitation scheme for climate and data-assimilation purposes.. *Quart. J. Roy. Met. Soc.*, **128(A)**, 229–258
- Louis, J. F. 1979 A parametric model of vertical fluxes in the atmosphere. *Boundary-Layer Meteorology*, **17**, 187–202
- Mellor, G. L. and Yamada, T. 1974 A Hierarchy of Turbulence Closure Models for Planetary Boundary Layers. *J. Atmos. Sci.*, **31**, 1791–1806
- Neggers, R. A. J., Siebesma, A. P. and Jonker, H. J. J. 2002 A Multiparcel Model for Shallow Cumulus Convection.. *J. Atmos. Sci.*, **59**, 1655–1668
- Neggers, R. A. J., Siebesma, A. P., Lenderink, G. and Holtslag, A. A. M. 2003 An evaluation of mass flux closures for diurnal cycles of shallow Cumulus. Accepted by Mon. Wea. Rev.
- Rasch, P. J. and Kristjánsson, J. E. 1998 A comparison of the CCM3 model climate using diagnosed and predicted condensate parameterizations. *J. Climatol.*, **11**, 1587–1614
- Ricard, J. L. and Royer, J. F. 1993 A statistical cloud scheme for use in an AGCM. *Ann. Geophysicae*, **11**, 1095–1115
- Roeckner, E., Bengtsson, L., Christoph, M., Claussen, M., Dumenil, L., Esch, M., Giorgetta, M., Schlese, U. and Schulzweida, U. 1996 ‘The Atmospheric general circulation model ECHAM-4: Model description and simulation of present-day climate’. Tech. Rep. 218 Max-Planck-Institut für Meteorologie (Bundesstrasse 55, D-20146 Hamburg F.R. Germany)
- de Roode, S. R. and Duynkerke, P. G. 1997 Observed Lagrangian transition of stratocumulus into cumulus during ASTEX: mean state and turbulence structure. *J. Atmos. Sci.*, **54**, 2157–2173
- van Salzen, K. and McFarlane, N. A. 2002 Parameterization of the Bulk Effects of Lateral and Cloud-Top Entrainment in Transient Shallow Cumulus Clouds.. *J. Atmos. Sci.*, **59**, 1405–1430
- Sanchez, E. and Cuxart, J. 2003 A buoyancy-based mixing length proposal for cloudy boundary layers. QJRMS (EUROCS special issue)
- Siebesma, A. P., Bretherton, C. S., Brown, A., Chlond, A., Cuxart, J., Duynkerke, P. G., Jiang, H., Khairoutdinov, M., Lewellen, D., Moeng, C.-H., Sanchez, E., Stevens, B. and Stevens, D. E. 2003 A large eddy simulation intercomparison study of shallow cumulus convection. *J. Atmos. Sci.*, **60**, 1201–1219
- Siebesma, A. P. and Cuijpers, J. W. M. 1995 Evaluation of parametric assumptions for shallow cumulus convection. *J. Atmos. Sci.*, **52**, 650–666

- Siebesma, A. P. and Holtslag, A. A. M. 1996 Model Impacts of Entrainment and Detrainment Rates in Shallow Cumulus Convection. *J. Atmos. Sci.*, **53**, 2354–2364
- Siebesma, A. P. and Teixeira, J. 2000 ‘An advection-diffusion scheme for the convective boundary layer, description and 1d-results’. Pp. 133–136 in Proceedings of 14th Symposium on Boundary Layers and Turbulence, Aspen, USA. American Meteorological Society
- Stevens, B. 2000 Quasi-steady analysis of a PBL model with an eddy-diffusivity profile and non-local fluxes. *Mon. Wea. Rev.*, **128**, 824–836
- Stevens, B., Ackerman, A. S., Albrecht, B. A., Brown, A. R., Chlond, A., Cuxart, J., Duynkerke, P. G., Lewellen, D. C., Macvean, M. K., Neggers, R. A. J., Sanchez, E., Siebesma, A. P. and Stevens, D. E. 2001 Simulations of trade-wind cumuli under a strong inversion. *J. Atmos. Sci.*, **58**, 1870–1891
- Sundqvist, H., Berge, E. and Kristjansson, J. E. 1989 Condensation and Cloud Parameterization Studies with a Mesoscale Numerical Prediction Model. *Mon. Wea. Rev.*, **117**, 1641–1657
- Teixeira, J. 1999 ‘The impact of increased boundary layer vertical resolution on the ECMWF forecast system’. Tech. Rep. 268 ECMWF (Shinfield Park, RG2 9AX Reading, United Kingdom)
- Teixeira, J. 2001 Cloud fraction and relative humidity in a prognostic cloud fraction scheme. *Mon. Wea. Rev.*, **129**, 1750–1753
- Tiedtke, M. 1989 A comprehensive mass flux scheme for cumulus parameterization in large-scale models. *Mon. Wea. Rev.*, **117**, 1779–1800
- Tiedtke, M. 1993 Representation of Clouds in Large-Scale Models. *Mon. Wea. Rev.*, **121**, 3040–3061
- Tompkins, A. 2002 A prognostic parameterization for the subgrid-scale variability of water vapor and clouds in large-scale models and its use to diagnose cloud cover. *J. Atmos. Sci.*, **59**, 1917–1942
- Troen, I. and Mahrt, L. 1986 A simple model of the atmospheric boundary layer: sensitivity to surface evaporation. *Boundary-Layer Meteorology*, **37**, 129–148
- Uden, P., Rontu, L. and 24 Co-authors 2002 ‘HIRLAM-5 scientific documentation.’. Tech. rep. SMHI (S-601 76 Norrköping, Sweden)